A Non-Invasive Metamaterial Characterization System Using Synthetic Gaussian Aperture

***Jae-Young Chung*, Kubilay Sertel, John L. Volakis**

ElectroScience Laboratory, Department of Electrical and Computer Engineering, The Ohio State University, Columbus, Ohio, USA. e-mail: chung.275@osu.edu, sertel.1@osu.edu, volakis@ece.osu.edu

Abstract

A new free-space measurement approach for characterizing RF materials and metamaterials over a wide frequency range is presented. As an alternative to the widely used non-invasive spot-focused horn pair system, the proposed technique synthetically generates a Gaussian beam with a tight spot focused on the sample under test. Much like synthetic aperture radar post-processing, individually measured responses are used to generate a virtual Gaussian aperture. Accordingly, the bandwidth limitations originated from the difficulties in fabricating lenses of the conventional system can be resolved. Theoretical studies and design configurations for the new system employing both planar and spherical virtual apertures are discussed. The technique is validated using a dielectric slab of known permittivity. Furthermore, a rather complex metamaterial slab made of uniaxial material layers is characterized. Measured results show excellent agreement with computed data demonstrating the potential of the method.

1. Introduction

Non-invasive characterization of homogenized electromagnetic properties of composite materials has recently drawn renewed attention due to the advances in periodic composites that exhibit unique dispersion behavior [1]. Commonly termed as metamaterials, these composites have extraordinary properties dramatically improving the performance of microwave components and antenna elements. However, the incorporation of such metamaterials as substrates and/or superstrates requires an accurate characterization of their electromagnetic properties.

Among the widely used material characterization techniques [2], resonant cavity method is the most accurate, however, invasive reshaping of the sample to fit into the measurement fixture is required. Furthermore, the measurement is only possible in the very close vicinity of the resonant frequency. An open-ended coaxial probe measurement operates over broader bandwidth without exhaustive sample preparation, but a good contact between the sample and probe is needed to eliminate the air-gap effects. Alternatively, free-space measurement method, which is one of the transmission/reflection methods, is highlighted due to its contactless and non-invasive feature. Free-space measurement (FSM) system characterizes materials by measuring S-parameters for a pair of antennas facing each other with the sample placed in the middle of their line of sight (see Fig. 1a). In particular, it consists of a pair of horn antennas corrected by two dielectric lenses placed over their apertures to have a common focal point on the sample surface [3]. Hence, the radiated field from the transmitting horn is focused by the lens into a Gaussian beam with its spot at the sample location. Utilization of this collimated Gaussian beam minimizes diffractions from the edges of the sample. Furthermore, the wave fronts are almost planar throughout the sample, allowing a simple plane-wave transmission/reflection theory for determining the material parameters.

Unfortunately, existing FSM system has major disadvantages for a wideband characterization of materials. First, its operation bandwidth is limited by antennas used. Furthermore, the antenna separation must be large enough (to satisfy paraxial limits of the Gaussian beam solution) and the lenses used to collimate the transmitted and received fields have to be very precise to eliminate wave front aberrations (such as spherical aberrations). This entails large antenna apertures and lenses. Such lenses are also very costly to custom-manufacture for each frequency band, especially, for low frequency characterization.

As an alternative, herewith we propose a new technique that is based on synthetic aperture antennas/arrays. The synthetic nature of the collimated beam allows for post processing of the collected data to remove the abovementioned shortcomings. The simple idea is to replace a spot-focused horn with a synthetic aperture, as depicted in Fig. 1b. The virtual surface of the synthetic aperture is simply scanned using a small, low-profile probe antenna. The measured S-parameter values are then stored on the network analyzer, which are subsequently processed to synthesize a very large properly weighted aperture (i.e. reproducing the Gaussian beam). In this paper, we demonstrate the proposed technique by measuring the transmission coefficient (S_{21}) using both planar and spherical scanning setups through a dielectric slab with known permittivity and a rather complex periodic assembly of material layers realizing a degenerate band edge (DBE) crystal.

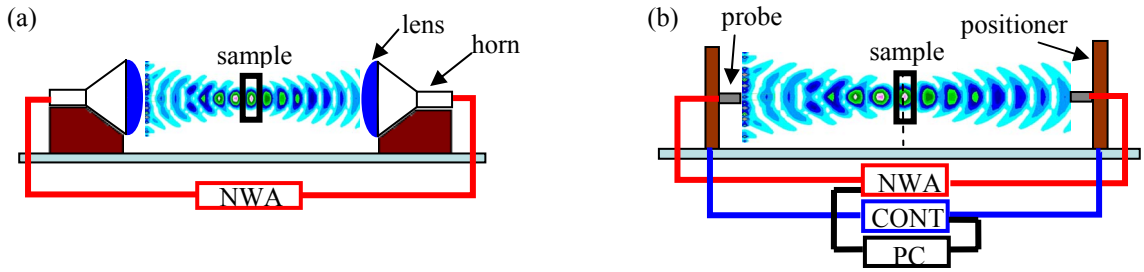

Figure 1. Two free-space measurement systems (a) spot-focused horn pair (b) the proposed synthetic aperture system with planar scanning x-y tables. NWA, CONT, and PC refer to network analyzer, controller, and personal computer.

2. Synthesizing the Virtual Gaussian Aperture

The main goal of the proposed measurement system is the reproduction of a large Gaussian distributed aperture that radiates the desired Gaussian beam focused on the sample under test. The flow chart shown in Fig. 2 describes the steps from collecting the individual data to extracting the material properties. By properly weighting and synthesizing individually scanned data, it is possibly to reproduce a planar or a spherical aperture that generates the correct Gaussian beam illumination (as illustrated in Fig. 3). For collecting the S_{21} data, we demonstrate the applicability of both a planar scan (Fig. 3a) and a polar-pointing spherical scan (Fig. 3b) using a linear x-y table (Fig. 4a) and the spherical scanning capability (Fig. 4b) in the anechoic chamber at the ElectroScience Laboratory of the Ohio State University.

The required scanning parameters can be defined by Gaussian beam parameters (see Fig. 5). As is widely known the complex magnitude of the Gaussian beam (U) involves the parameters: waist (W_0), depth of focus (z_0), beamwidth (W), radius of curvature (R), and Guoy phase (ζ) as depicted in Fig. 5. These are given as

$$U(\boldsymbol{r}) = \frac{1}{jz_0}\frac{W_0}{W(z)}\exp\left[-\frac{\rho^2}{W^2(z)}\right]\exp\left[-jkz - jk\frac{\rho^2}{2R(z)} + j\varsigma(z)\right], \quad (1)$$

$$W(z) = W_0\left[1+\left(\frac{z}{z_0}\right)^2\right]^{1/2}, \quad (2) \qquad R(z) = z\left[1+\left(\frac{z_0}{z}\right)^2\right], \quad (3) \qquad \zeta(z) = \tan^{-1}\left(\frac{z}{z_0}\right), \quad (4) \qquad z_0 = \frac{\pi W_0^2}{\lambda}, \quad (5) \qquad \theta_0 = \frac{\lambda}{\pi W_0}, \quad (6)$$

where $\rho^2 = x^2 + y^2$ and λ is the wavelength. In order to start designing the proper aperture size and number of samples required to synthesize the desired Gaussian beam, the minimum waist size W_0 must be specified. For example, if the minimum spot size is chosen to be as large as the wavelength λ, the divergence angle turn out to be $\theta_0 = 1/\pi$ radians. This is in accordance with the validity constraints of the paraxial wave equation. Secondly, the minimum scan area can be chosen to cover 99% of the total energy. This is required to avoid any contribution from artificial diffractions at the synthetic aperture edges. In Fig. 5, the area range defined by $W(z_a)$ or θ_0 includes 86% of the energy. On the other hand, the increased area W_s or θ_s, which is 1.5 times of $W(z_a)$ or θ_0, covers 99% of the energy. For instance, a $2W_s$ x $2W_s$ area must be scanned for the planar setup and the angular range coverage ($-\theta_s$, θ_s) is required for the spherical scan. Finally, scanning intervals (number of samples) are determined by Nyquist sampling rate. The rules to satisfy Nyquist sampling rate for planar and spherical scan are given as

$$\Delta x = \Delta y < \frac{\lambda}{2}, \quad (7) \qquad \Delta\theta = \Delta\phi < \frac{\lambda}{2(a+\lambda)}, \quad (8)$$

where a refers to the circumscribing radius of the sample under test. Based on above discussions the minimum scan areas and maximum scan intervals must be chosen with respect to the lowest and highest frequencies, respectively, for broadband measurements.

Calibration of the synthetic channel is done with respect to the no-sample measurements (i.e. free-space channel), and multiple reflections between the Rx-probe and sample are filtered out by means of time-domain gating using a Hanning window. An important step in the post-processing is correcting the phase errors prior to the weighting and summation of the individual data. Such errors are due to positioning uncertainties during planar or spherical scans and/or phase center migrations as Rx-probe is rotated in the spherical scan. These errors are compensated by comparing the measured and calculated phase responses for the given measurement geometry. After geometrical error correction, each measured data is multiplied with the corresponding Gaussian weights obtained from (1)-(6). Adding all the properly weighted data provides a single S_{21} for the synthetic channel. This transmission coefficient is compared with the analytical plane-wave transmission coefficient to extract the permittivity of the material sample.

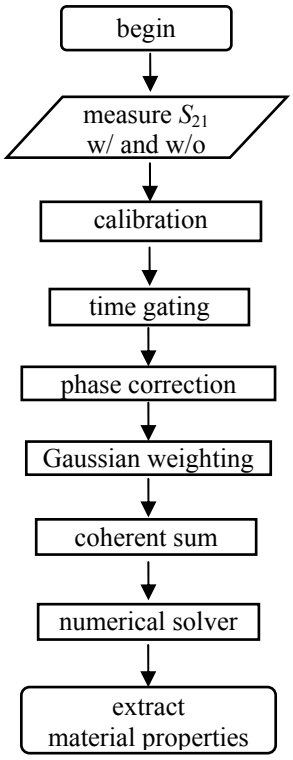

Figure 2. Flow chart of new free-space measurement procedure.

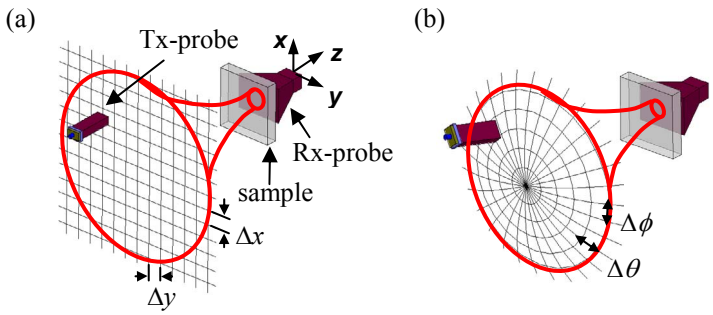

Figure 3. Different scanning methods. (a) planar scan and (b) spherical scan.

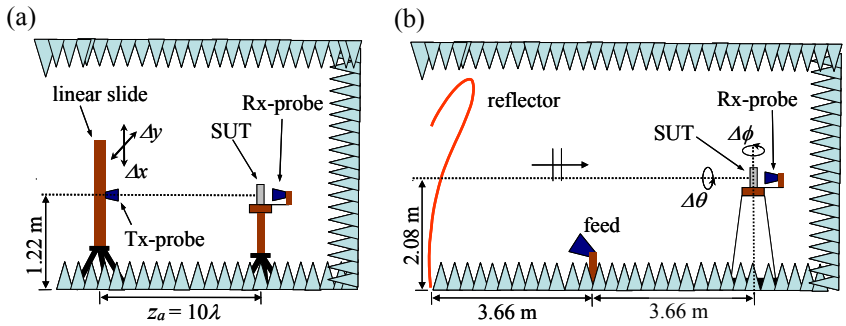

Figure 4. Measurement setups of (a) planar scan and (b) spherical scan.

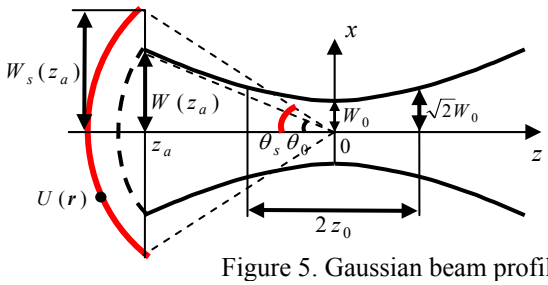

$$W_s = 1.5W \approx 1.5\frac{W_0}{z_0}z_a$$

$$\theta_s = 1.5\theta_0 \approx 1.5\frac{\lambda}{\pi W_0}$$

(for $z_a >> z_0$)

Figure 5. Gaussian beam profile.

3. Measurement Examples

We first validated our measurement technique by characterizing a dielectric slab with a known permittivity of $\varepsilon_r = 9.0$ using the planar and spherical scanning systems. Measured data was collected in the X-band (8-12 GHz) using a frequency sweep of 401 points on an Agilent 8722ET network analyzer. A pair of X-band standard gain horns was used as transmitting and receiving probe for planar scan, while 2-18 GHz double ridge horn was used as the feed of reflector for spherical scan. The scanning parameters were calculated in order to satisfy the reconstruction conditions discussed in Section 2. Parameters such as $W_s = 37.5$ cm, $\Delta x = \Delta y = 1.25$ cm were used for planar scan, and $\theta_s = 30$ and $\Delta\theta = \Delta\phi = 5$ degree were used for spherical scan. Fig. 6 and Fig. 7 show the magnitude and phase of the calculated S_{21} and measured S_{21} by the synthesized Gaussian beam. Also shown is the 'face-to-face' data indicating the S_{21} measurement for the line-of-sight data (i.e. $x = y = 0$ and $\theta = \phi = 0$ for planar and spherical scan) to demonstrate the effects of diffractions and multiple reflections. The agreement with measured and calculated data is impressive, especially for spherical scanned case. Note that no phase correction step was necessary for spherical scan measurement due to its stable setup over the measurement time. Based on the measured S_{21} data, the extracted permittivity had a maximum 4.3% error for planar scan and 2.3% error for spherical scan.

Furthermore, we characterized the transmission behavior for a DBE slab presented in [4] with the new system. The measurement was performed on spherical scanning set-up with the same scanning parameters as the previous example, except for the frequency range of 7-14 GHz. The measured and calculated results are shown in Fig. 8 with very good agreements in both magnitude and phase. Fabry-Perot transmission peaks are clearly identified at 8, 10.25, and 13.4 GHz corresponding to regular band edge (RBE), degenerate band edge (DBE), and double band edge (DdBE), respectively.

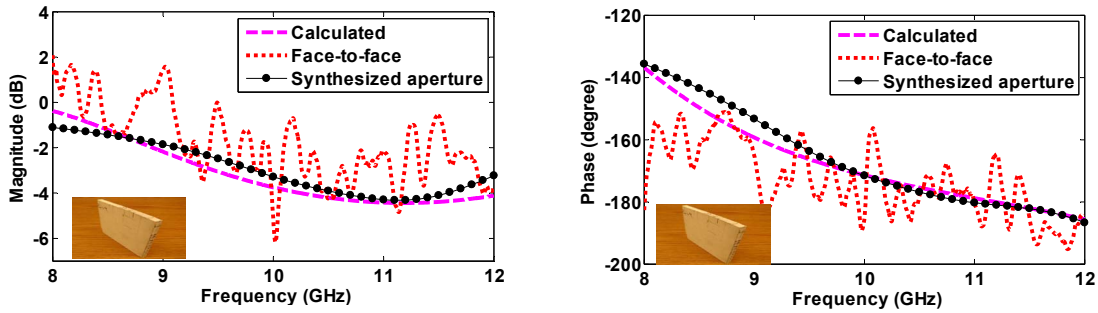

Figure 6. S_{21} data of $\varepsilon_r = 9.0$ dielectric slab (10.16 x 10.16 x 0.67 cm^3) characterized by planar scanning method.

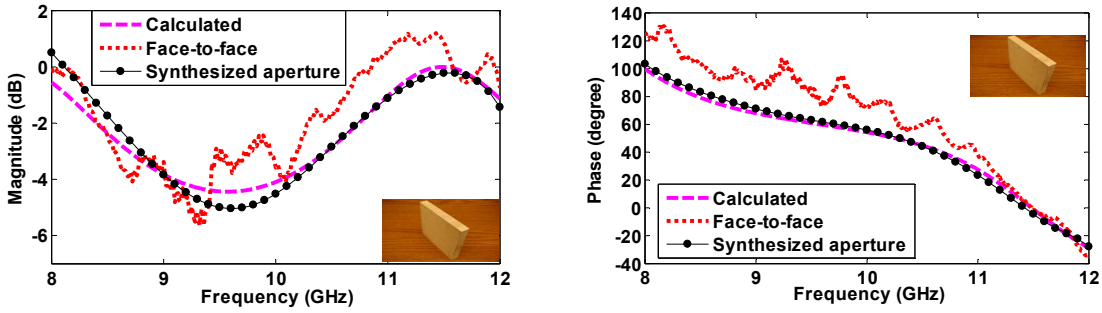

Figure 7. S_{21} data of $\varepsilon_r = 9.0$ dielectric slab (10.16 x 10.16 x 1.3 cm^3) characterized by spherical scanning method.

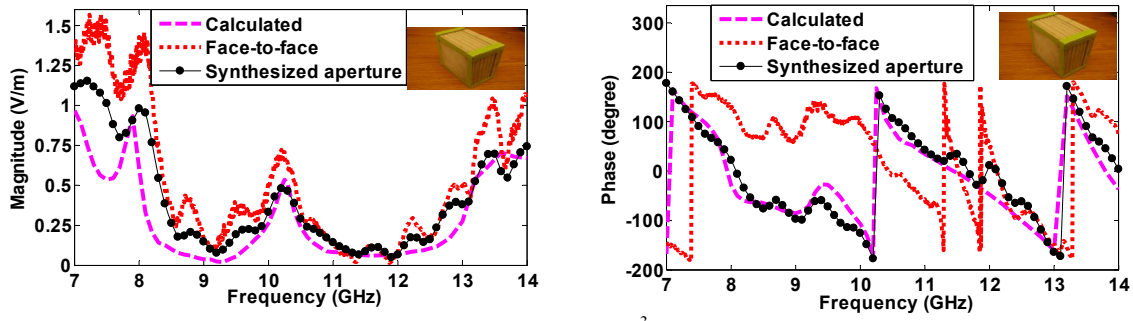

Figure 8. S_{21} data of DBE structure (10.9 x 10.9 x 5.8 cm^3) characterized by spherical scanning method.

4. Conclusion

We described a new wideband material characterization technique that can be used to accurately measure the dielectric permittivity as well as transmission characteristics of periodic crystal metamaterials. The measurement system is based on a virtual transmitting aperture that is synthesized to produce a Gaussian beam spot-focused on the sample under test. It is worth noting that the new system set-up can easily be retrofitted to existing planar and spherical scanning apparatuses available in most EM facilities.

5. References

1. V. Varadan and A. R. Tellakula, "Effective properties of split-ring resonator metamaterials using measured scattering parameters: Effect of gap orientation," *J. Appl. Phys.*, 100, 034910, 2006.
2. L. F. Chen, C. K. Ong, C. P. Neo, V. V. Varadan, and V. K. Varadan, *Microwave Electronics: Measurement and Materials Characterization*, Wiley, Chichester, 2004.
3. D. K. Ghodgaonkar, V. V. Varadan, and V. K. Varadan, "Free-space method for measurement of dielectric constants and loss tangents at microwave frequencies," *IEEE Trans. Instrum. Meas.,* 37(3), 789-793, 1989.
4. S. Yarga, K. Sertel, and J. L. Volakis, "Degenerate band edge crystals for directive antennas," *IEEE Trans. Antennas Propag.,* 56(1), 119-126, 2008.